Brief Communication Communication brève

Pure cystine and urate calculi can be clearly visible using survey digital radiography

Esther Nell, Stephen Q. Garofolo, Christopher Ober

Abstract

Objective
Cystine and urate calculi are usually considered nonradiopaque to faintly radiopaque. The present study was designed to examine that clinical assumption.

Animals and samples
Two canine cases in which these types of calculi were radiopaque and clearly apparent *in vivo* on survey digital radiography are described. Subsequently, 35 calculi from 34 dogs were evaluated.

Procedures
The densities of cystine and urate calculi, as determined *in vitro* with computed tomography, were compared to other pure calculi, and mixed or compound calculi, to explore the relative attenuation characteristics.

Results
Computed tomographic density values expressed as Hounsfield units (HU) for silica, cystine, urate, and struvite were not different from one another ($P > 0.2$ for all ordered differences), whereas the HU range for calcium oxalate was higher (all $P < 0.001$).

Conclusions and clinical relevance
This study supports the ability to recognize cystine and urate calculi through digital radiography. As density is one of the main factors determining radiographic attenuation, and perhaps because of better contrast resolution of digital radiography, direct comparison between screen-film and digital radiography was not performed.

Résumé

Les calculs de cystine et d'urate purs peuvent être clairement visibles à l'aide de la radiographie numérique standard

Objectif
Les calculs de cystine et d'urate sont généralement considérés comme étant non radio-opaques ou faiblement radio-opaques. La présente étude a été conçue pour examiner cette hypothèse clinique.

Animaux et échantillons
Deux cas de chiens chez qui ces types de calculs étaient radio-opaques et clairement apparents *in vivo* à la radiographie numérique sont décrits. Par la suite, 35 calculs provenant de 34 chiens ont été évalués.

Protocole
Les densités des calculs de cystine et d'urate, déterminées *in vitro* par tomodensitométrie, ont été comparées à celles d'autres calculs purs et de calculs mixtes ou composés pour explorer davantage les caractéristiques d'atténuation.

Department of Veterinary Clinical Sciences, College of Veterinary Medicine, University of Minnesota, 1365 Gortner Avenue, St. Paul, Minnesota 55108, USA.

Address all correspondence to Dr. Esther Nell; e-mail: e.nell.dvm@gmail.com

Résultats
Les valeurs de densité à la tomodensitométrie exprimées en unités Hounsfield (HU) pour les calculs de silice, de cystine, d'urate et de struvite n'étaient pas différentes les unes des autres ($P > 0,2$ pour toutes les différences évaluées), alors que celles pour les calculs d'oxalate de calcium étaient plus élevées ($P < 0,001$ dans tous les cas).

Conclusions et portée clinique
Cette étude indique que les calculs de cystine et d'urate peuvent être vus à la radiographie numérique, étant donné que la densité est l'un des principaux facteurs déterminant l'atténuation radiographique, et peut-être en raison de la meilleure résolution de contraste de la radiographie numérique, bien qu'une comparaison directe entre la radiographie numérique et la radiographie sur film avec écran n'ait pas été effectuée.

Urolithiasis is common in dogs (1). Cystine and urate urinary calculi are considered to be nonradiopaque to faintly radiopaque (2). The main goal of this brief communication is to report 2 cases of *in vivo* survey digital radiographic identification of cystine and urate urinary calculi in 2 canine patients. There are few peer-reviewed reports of cystine or urate calculi detected *in vivo* on survey radiography in dogs and cats, with even fewer available radiographic images (3–6). A secondary aim is to report computed tomographic attenuation values of cystine and urate calculi compared to other calculi to explore the role of density in the radiographic findings described *in vivo*.

The first case is a 2-year-old, intact male American pit bull terrier that was presented to the University of Minnesota 2 times over a period of 6 mo for stranguria. At each episode, multiple small calculi were identified within the urinary bladder on survey digital radiography (Vet Ray; Sedecal, Arlington Heights, Illinois, USA and Canon CXDI unspecified model; Melville, New York, USA) (Figure 1 A). Urethral calculi were suspected, although not definitively identified due to soft tissue superimposition. Following retropulsion and stabilization, the calculi were subsequently removed *via* cystotomy and analyzed to be 100% cystine in both episodes.

The second case is an 8-year-old, neutered male Dalmatian dog that was presented with vomiting, anorexia, and straining to urinate. An 11 × 6 mm calculus was clearly identified within the plane of the urethra on survey digital radiography (Vet Ray; Sedecal) (Figure 1 B). Two smaller urethral calculi, radiographically faint urinary bladder calculi, and a nephrolith were also seen. Following retropulsion and stabilization, calculi were removed *via* cystotomy and analyzed to be 100% ammonium urate. All calculi analyses were conducted by the Minnesota Urolith Center (University of Minnesota, St. Paul, Minnesota, USA).

To further explore the relationship between radiographic opacity and material density, several groups of calculi were evaluated *in vitro* using computed tomography (CT). The calculi were provided by the Minnesota Urolith Center. A urolith without a nidus, shell, or surface crystal layer that contained ≥ 70% of 1 type of mineral was identified by that mineral. A urolith with < 70% of 1 mineral but without a nidus, shell, or surface crystals was referred to as a mixed urolith. A urolith with an identifiable nidus and/or stone with ≥ 1 surrounding layer(s) of different mineral composition was called a compound urolith (7).

Uroliths were placed into individual plastic cups that had been partially filled with a clear gelatin substrate, allowing the uroliths to rest approximately 5 mm above the bottom of the cups. Uroliths were then covered with 0.9% saline (8). Cups were arranged in a grid and then scanned using a helical CT scanner (Toshiba Aquilion 64 CFX CT; Toshiba, Tustin, California, USA) at 120 kV and 100 mAs and reconstructed in 0.5-mm slices using a soft tissue algorithm. Freeform regions of interest (ROI) were drawn on each sample calculus or the largest calculus in a sample of multiple calculi to obtain average Hounsfield units (HU), evaluated with a window level of 25 and a window width of 350. The ROI were drawn just within the visible calculi borders to ensure that the surrounding saline was not inadvertently included in the measurements.

Computed tomographic density values (HU) were evaluated using statistical software (JMP Pro 13.2.1; SAS Institute, Cary, North Carolina, USA). Means and standard deviations of HU for all non-mixed, non-compound calculi types with at least 3 specimens were calculated. One-way analysis of variance (ANOVA) procedures were performed to compare HU values among the groups of calculi, and when the ANOVA demonstrated significant differences among calculi, differences between pairs of groups were assessed using the Tukey-Kramer HSD Experiment-wise test. Statistical significance for analyses was set at $P < 0.05$.

Thirty-five calculi samples were obtained from 34 dogs. Two of the cystine samples were obtained from the first case described in this report. Twenty-nine of the samples were analyzed to be 100% pure in composition, including calcium oxalate ($n = 9$), cystine ($n = 6$), urate ($n = 3$), struvite ($n = 3$), silica ($n = 3$), xanthine ($n = 1$), potassium magnesium phosphate (PMP, $n = 1$), and calcium phosphate carbonate (CPC, $n = 1$). An additional struvite sample had a nidus composed of 5% CPC and a brushite sample had a nidus of 15% calcium oxalate; these samples did not meet criteria for categorization of mixed or compound. The remaining 6 samples were mixed or compound in composition.

Hounsfield units ranged from 219 to 1848, depending on the calculus type (Table 1). Brushite and calcium oxalate were the highest attenuating calculi, similar to previous results (8,9). The HU ranges for struvite, cystine, and urate in this study were similar to previous results (8,9). The HU obtained for the PMP, CPC, brushite, and xanthine samples were excluded from statistical analyses as only 1 sample for each of these calculi types was available. The HU obtained for silica, cystine, urate, and struvite were not different from one another ($P > 0.2$ for all ordered differences). To the authors' knowledge, measured HU of silica calculi has not been reported in veterinary medicine.

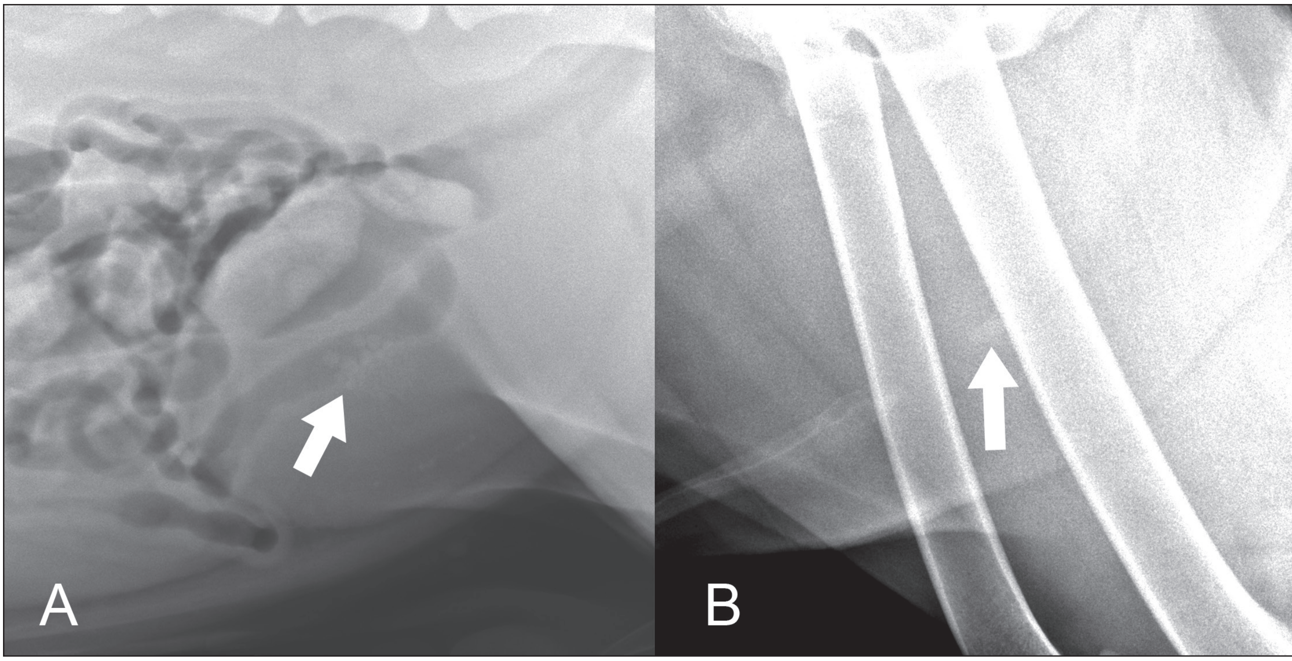

Figure 1. Survey radiographs of dogs with cystine and urate urolithiasis. A – Cystine urinary bladder calculi (arrow) (kVp 81, mAs 10.2). B – A urate urethral calculus (arrow) (kVp 92, mAs 3.2).

Table 1. Hounsfield units determined for each type of calculus. For calculus types with multiple samples, results are reported as range (median).

Type	Hounsfield units
Calcium oxalate	969 to 1496 (1141)
Struvite	487 to 643 (637)
Urate	431 to 539 (431)
Cystine	344 to 544 (427)
Silica	333 to 535 (408)
Brushite	1740
CPC	1123
PMP	908
Xanthine	219
Mixed/compound	332 to 1848

PMP — Potassium magnesium phosphate; CPC — Calcium phosphate carbonate.

The HU range for calcium oxalate was different from silica, cystine, urate, and struvite calculi (all $P < 0.001$). The range of HU for mixed and compound calculi was broad and overlapped with ranges obtained for other calculi types. For reference, distilled water is defined as having a value of 0 HU, the reported mean HU of canine urine is 35.6 and the HU of non-contrast enhanced liver is approximately 50 to 70 (10,11).

This report provides 2 examples in which calculi types historically considered to be non-radiopaque were readily identified *in vivo* on survey digital radiography. When evaluating the densities of representative cystine and urate calculi as determined with CT, there was no difference between the density of cystine and urate calculi and reportedly radiopaque calculi. This supports the ability to recognize cystine and urate calculi radiographically, as density is 1 of the main factors determining radiographic attenuation (12). A previous study of urinary calculi obtained from dogs demonstrated poor accuracy of detection of cystine and urate calculi *in vitro* when evaluated using screen-film radiography (13). It is speculated that the relatively radiopaque nature of the calculi of the 2 *in vivo* cases herein is due in part to the greater contrast resolution of digital radiography compared to screen-film systems, acknowledging that direct comparison between screen-film and digital radiography was not made in these 2 cases (14). The greater contrast resolution in digital radiography is related to the wider dynamic range associated with digital imaging receptors when compared to the silver halide crystal system of screen-film radiography. The effect of other variables such as calculus size is also acknowledged (13). Large-scale, ideally *in vivo,* studies evaluating the accuracy of survey digital radiography (potentially with comparison to screen-film radiography) in the diagnosis of various types and sizes of urolithiasis are warranted for further exploration of this subject, as *in vivo* prediction of urolith composition is used to guide case management (15).

Acknowledgments

The authors thank the Minnesota Urolith Center which provided urolith analysis at no cost and the support from Hill's Pet Nutrition and voluntary donors. CVJ

References

1. Hesse A. Canine urolithiasis: Epidemiology and analysis of urinary calculi. J Small Anim Pract 1990;31:599–604.
2. Marolf A. Urinary bladder. In: Thrall D, ed. Textbook of Veterinary Diagnostic Radiology. 7th ed. Philadelphia, Pennsylvania: Saunders, 2017:851.
3. Grauer G. Cystine urolithiasis. Clinician's Brief 2014;12:71–73.
4. Butty E, Bua A, Vanstone N, Dunn M. Retained laser fiber in the nidus of a recurrent cystine urolith in an intact male English bulldog. Can Vet J 2019;60:29–32.
5. Grauer G. Ammonium urate urolithiasis. Clinician's Brief 2014;12: 51–55.

6. Collins R, Birchard S, Chew D, Heuter KJ. Surgical treatment of urate calculi in Dalmatians: 38 cases (1980–1995). J Am Vet Med Assoc 1998;213:833–838.
7. Osborne C, Clinton C, Bamman L, Moran H. Prevalence of canine uroliths: Minnesota Urolith Center. Vet Clin North Am Small Anim Pract 1986;16:27–44.
8. Pressler BM, Mohammadian LA, Li E, et al. In vitro prediction of canine urolith mineral composition using computed tomographic mean beam attenuation measurements. Vet Radiol Ultrasound 2004;45:189–197.
9. Nykamp S. Dual-energy computed tomography of canine uroliths. Am J Vet Res 2017;18:1150–1155.
10. Zwingenberger A, Carrade Holt D. Computed tomographic measurement of canine urine concentration. Can Vet J 2017;58:180–182.
11. Ohlerth S, Scharf G. Computed tomography in small animals — Basic principles and state of the art applications. Vet J 2007;173:254–271.
12. Curry T, Dowdey J, Murry R. Christensen's Physics of Diagnostic Radiology. 4th ed. Philadelphia, Pennsylvania: Lippincott Williams & Wilkins, 1990.
13. Weichselbaum R, Feeney D, Jessen C, Osborne C, Dreyster V, Holte J. Urocystolith detection: Comparison of survey, contrast radiographic, and ultrasonographic techniques in an in vitro bladder phantom. Vet Radiol Ultrasound 1999;40:386–400.
14. Weatherburn G, Davies J. Comparison of film, hard copy computed radiography (CR) and soft copy picture archiving and communication (PACS) systems using a contrast detail test object. Br J Radiol 1999; 72:856–863.
15. Lulich JP, Berent AC, Adams LG, Westropp JL, Bartges JW, Osborne CA. ACVIM Small Animal Consensus Recommendations on the treatment and prevention of uroliths in dogs and cats. J Vet Intern Med 2016;30:1564–1574.